Fiber Laser Intracavity Absorption Spectroscopy measurements of combustion product concentration and temperature

A. Fomin[1], T. Zavlev[1], V.Tsionsky[1], I. Rahinov[2], S. Cheskis[1*]

[1] School of Chemistry, Tel Aviv University, Tel Aviv 69978, Israel.
[2] Department of Natural Sciences, The Open University of Israel, Raanana 4353701, Israel

Abstract

A method for the simultaneous measurement of carbon dioxide (CO_2) and carbon monoxide (CO) absolute concentrations and temperature using fiber laser intracavity absorption spectroscopy (FLICAS) was developed. FLICAS uses an erbium-doped broadband laser capable of being tuned in the range 6350 - 6450 cm^{-1}. The range 6390 - 6410 cm^{-1}, which is emitted by the laser without tuning, allows for simultaneous observation of the CO, and CO_2 spectra. Truly simultaneous observation of these spectra is possible during one laser pulse with duration as short as 3.7 μs. The experiments were performed in a temperature and flow-controlled cell in order to evaluate the accuracy of the concentration and temperature measurements from 296 to 1200 K. The measured spectra of CO and CO_2 are well described by the HITRAN database, allowing for accurate and simultaneous determination of CO, CO_2 and temperature. The temperature is evaluated using the CO_2 spectrum, which includes many "hot" transitions. The CH_4 HITRAN data are deficient at high temperatures, so this method only allows for the evaluation of methane concentrations at room temperature. The FLICAS spectra of the"hot" water lines in flames allow to evaluate correctly the flame temperature.

1 Introduction

The ability to simultaneously monitor multiple species is of utmost importance. In many cases, the concentration ratio is more informative than the absolute concentrations of individual components. This is due to the dependence of the latter on possible dilution by other gases at the point of measurement. For instance, the ratio of CO_2 to CO is a well-known indicator of the completeness of combustion, so measurement of both gases is often required in technical combustion equipment or its exhaust gases. Accurate and simultaneous measurement of these gases, along with a precise temperature determination, is crucial to evaluating the environmental and performance aspects of combustion and gas-reforming devices.

Detection of CO and CO_2 concentrations has been accomplished by various techniques, most of which are based on tunable diode laser spectroscopy, abbreviated TDLAS [1–9]. Quasi-simultaneous multispecies monitoring can be accomplished with the fast laser wavelength scanning technique [4,10–12]. In the very recent work by Spearrin et al. [12] two mid-infrared quantum cascade lasers were used for simultaneous monitoring of CO and CO_2 in a scramjet combustor. For temperature measurement with this method one of the lasers is scanned through two lines of CO with different energies of the lower levels of the corresponding transitions. The sensitivity of 1000 ppm CO for temperature and concentration measurements was demonstrated. The use of two line method for temperature evaluation limits the dynamic range of these measurements and the scanning requirements results in time resolution of 10 ms. An alternative approach is based on spectroscopy employing broadband light sources such as superluminescent light-emitting diodes [13,14], multimode absorption spectroscopy, MUMAS [6], or intracavity laser absorption spectroscopy (ICLAS) [15–18] and its fiber laser-based version FLICAS [19,20]. Thomson et al. [6] used MUMAS for simultaneous detection of CO and CO_2. In spite of broadband multimode laser source used in MUMAS, it demands scanning of the cavity length that affects the temporal resolution. A multipass cell used to improve the sensitivity allowed maximal optical length of 10 m. Sensitivity of about 1500 ppm was demonstrated for CO at room temperature.

ICLAS and FLICAS allow truly simultaneous measurement of multiple spectral features with very high sensitivity. The spectral range of FLICAS for a erbium-doped fiber extends from 6200 cm^{-1} to 6550 cm^{-1} and includes the spectra of several molecules playing key roles in combustion and combustion-related pollutant formation and abatement: CO_2, CO, H_2O, H_2S, C_2H_2, HCN and OH [19,20]. Near-IR spectral range includes lines from overtone and combination transitions, which have relatively low intensity. On the other hand, these transitions often overlap, allowing for simultaneous monitoring of several species in one spectrum. Additional advantage of the $\sim$1.5 μm spectral range used in this work is the availability of relatively low cost equipment (optics, ccd) developed for telecom applications.

The intensity of absorption spectra varies strongly with temperature due to the temperature dependence of each molecule's Boltzmann factor and partition function. Therefore, even retrieving relative concentrations from the observed absorption spectra requires a very accurate temperature measurement. Ideally, we use a non-intrusive method to determine the temperature from the

*corresponding author: cheskis@post.tau.ac.il
Proceedings of the Eoropean Combustion Meeting 2015

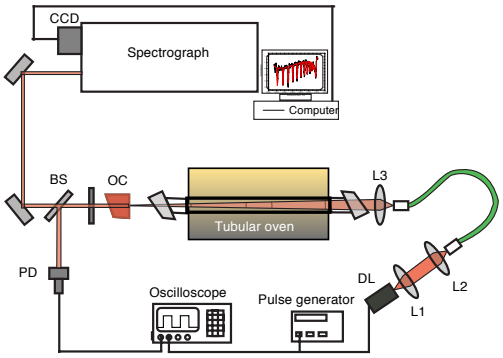

Fig. 1 Schematic of the experimental setup. L1, L2, and L3 are aspherical lenses, OC is an output coupler, BS is a beamsplitter, DL is a diode laser, and PD is a photodiode.

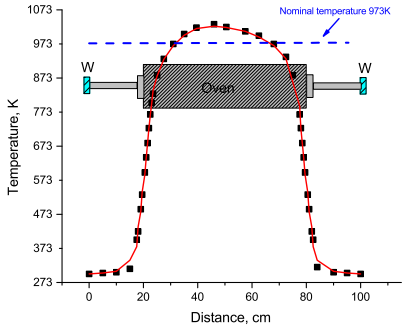

Fig. 2 Temperature distribution along the fuel cell for nominal oven temperature of 973 K, W are optical windows

same spectral information used for species concentration measurements.

The FLICAS method observes a relatively large section of the rovibrational spectrum, which makes it possible to measure both temperature and concentration simultaneously. An additional advantage of FLICAS is that it is insensitive to broadband losses, making it possible to work directly in harsh environments with strong broadband absorption or light scattering due to soot or other aerosol particles [18,21,22].

In our previous work [20] sensitivity of 25 ppm for CO at room temperature was demonstrated, as well as the ability to observe spectra of various stable molecules and radicals. In the present work, we report an application of FLICAS to measure concentrations of CO, CO_2, CH_4 separately and in their mixture at temperature range from 296 K to 1200 K, where in each case the temperature was extracted from the measured spectra of these molecules. The experiments were performed using a flow cell in a tubular oven, permitting us to create conditions with well-defined temperatures and concentrations. The goal of these experiments is to evaluate the feasibility and accuracy of FLICAS measurements for simultaneous temperature and concentration evaluation.

2 Experimental

The experimental setup, similar to the one described in our earlier publication [20], is shown in Fig. 1.

The fiber laser intracavity spectrometer is based on the external cavity erbium-doped fiber laser, which is optically pumped by a single-mode diode laser operating at 980 nm (S-980-9mm-0350, Axcel Photonics). The fiber used (R37PM01, OFS Fitel) is a single-mode polarization maintaining Er^{3+}-doped silica fiber.

The laser emission spectrum can be tuned by translating lens L3 along the optical axis, exploiting the effect of chromatic aberration. The output coupler (OC) is an external plane dielectric mirror with 5% transmission. It is wedged by 10^o to avoid interferometric fringes. The spectrum of the laser radiation is analyzed by a high resolution 1.25 m spectrograph, with a 100 grooves/mm echelle grating operating in the 11th order of dispersion. The spectra are recorded by an IR linear CCD camera (1024 pixels of 25 μm, Sensors Unlimited SU1024LE) and stored in a computer. The dispersion of the spectrograph is 0.92 cm^{-1}/mm or 0.023 cm^{-1}/pixel.

The gas passes through a flow cell – a stainless steel tube 100 cm long, situated in a temperature-controlled tubular oven 60 cm long. The entire flow cell-oven assembly is placed inside the fiber laser cavity. The use of a relatively long tube is associated with the necessity to have fairly uniform temperature distribution along the optical path. The example of this temperature distribution measured by thermocouple along the tube is shown in fig. 2 for nominal temperature of 973 K. The temperature within of the 80% of the oven length deviates from the nominal value by $\pm$50K and drops sharply outside of the oven.

Antireflection coated glass windows (12.6 mm thick, 1^o wedge) at both sides of the tube are slightly tilted with respect to the optical axis. The temperature profile along the optical axis rises sharply at the edges of the heated part of the tube. Inside the oven, the temperature profile is nearly flat with less than 50 K deviations from the nominal oven temperature. The gas flows are adjusted by calibrated mass-flow controllers (1259, MKS instruments).

In FLICAS the light transmission at the absorption line wavelength is governed by the Beer-Lambert law [19,20]:

$$I(\nu,t) = I_0(t)\exp(-n\sigma(\nu)L_{eff}) \qquad (1)$$

where n is the concentration of absorbing molecules, $\sigma(\nu)$ is the absorption cross section, and L_{eff} is determined according to

$$L_{eff} = \frac{l}{L}ct_{gen} \qquad (2)$$

L is the total length of the cavity; l/L is the filling ratio, the fraction of the cavity filled by the absorber; c is the speed of light; and t_{gen} is the time of generation. The total optical length of the laser cavity with a 42-cm-long

erbium-doped fiber is L = 181 cm. At room temperature the filling ratio can be determined by the distance between the optical windows in the cell (l=105 cm), so the filling ratio l/L=0.58. In experiments at elevated temperatures the total length of the gas absorbing at the oven temperature is 60 cm, but absorption by the cold gas at the edges of the tube must also be taken into account.

Immediately after switching the pump laser above the threshold, the fiber laser displays strong relaxation oscillations which are characteristic of solid state lasers[23]. The durations of the first few relaxation peaks are much shorter than the peak separation. In these experiments, the duration of the pump pulse was chosen such that the pump power drops immediately after the process of laser generation begins. Therefore, only one relaxation peak of fiber laser power was observed. The generation time in this case approximately equals the time difference between the end of the pump pulse and the maximum of the fiber laser pulse. Note, that since the duration of the relaxation peak is rather short, most of the light enters the spectrograph at the time t_{gen}, and therefore the effective optical length L_{eff} is well-defined. We estimate the uncertainty in L_{eff} to be less than 10%. The generation time t_{gen} in our experiments was 3.7 μs, which corresponds under our conditions to an effective path length of 644 m.

3 Results and Dicussion

The full spectral range is obtained by tuning the laser with the L3 lens, as described in the Experimental section. The broadband emission of the laser at a fixed L3 position covers a narrower spectral range. The most of experiments in this work was performed in the 6390 - 6410 cm^{-1} spectral range. We chose this range based on the following criteria. First, it must allow simultaneous determination of the CO and CO_2 concentrations, with more sensitivity to CO since the CO_2 concentration is substantially higher in most applications. Second, the selected range must allow temperature measurements and hence include lines which behave differently as the temperature changes.

The spectral range used in this work complies with these requirements. In this range, CO can be measured with high sensitivity and the temperature can be determined from rotational lines with high J numbers in the CO_2 spectrum. The intensity of the CO spectrum in this spectral range is about 20 times higher than that of CO_2. As mentioned above, this can be considered an advantage for many practical applications, where trace amounts of CO have to be detected on top of a dominant CO_2 background.

The spectral lines in our experiments are broadened mainly by collisions, since the Doppler width is narrower than the Lorentzian collisional linewidth by at least a factor of five even at 1200 K. However, the apparatus linewidth accounts for additional broadening. Therefore, we use the following procedure for spectral simulation. After assigning the spectral lines, the spectra of individual molecules are simulated with the aid of HITRAN[24] or HITEMP[25] (for its CO_2 database), including collision broadening and line shift coefficients. The line intensity $S(T)$ at temperature T is calculated based on the line intensity at the reference HITRAN temperature $T_{ref} = 296K$:

$$S(T) = S(T_{ref})\frac{Q(T_{ref})\exp(-c_2E/T)}{Q(T)\exp(-c_2E/T_{ref})} \tag{3}$$

where E is the energy of the lower transition level, $Q(T)$ is the partition function from the HITRAN database, and c_2 is the second radiation constant = hc/k=1.4388 cm K. The correct wavenumber ν' corresponding to the spectral line is determined using the pressure shift δ of the transition:

$$\nu' = \nu + \delta * 1atm \tag{4}$$

Thus, the monochromatic cross section $\sigma(\nu)$ is given by

$$\sigma(\nu) = S(T)f(\nu', T, p, \gamma) \tag{5}$$

where $f(\nu', T, p, \gamma)$ is the Lorentzian lineshape function and p is pressure:

$$f(\nu', T, p, \gamma) = \frac{1}{\pi}\frac{\gamma(p,T)}{\gamma^2(p,T) + \nu'^2} \tag{6}$$

and the half linewidth $\gamma(p,T)$ is calculated using γ_{air} from HITRAN:

$$\gamma(p,T) = \left(\frac{Tref}{T}\right)^n \gamma_{air} * p \tag{7}$$

The coefficient n reflects the temperature dependence of the air-broadened halfwidth from HITRAN. The spectral baseline was simulated with a 5th-7th order polynomial. The Beer-Lambert law (Eq.(1)) was used to generate the resulting spectrum. In the next stage, the generated spectrum was convoluted with the instrumental lineshape function approximated by a Gaussian, using a LabVIEW code based on the fast Fourier transform algorithm.

The polynomial coefficients along with the temperature and molecule concentration(s) were evaluated using a nonlinear least squares fit (the Levenberg-Marquardt algorithm), with the aid of a homemade LabVIEW program.

Fig. 3 depicts measured and simulated spectrum of 2% CO diluted by nitrogen to a total pressure of 1 atm at a temperature of 298K. The best fit yields 1.9% CO concentration and a temperature of 302K.

The inset in Fig. 3 demonstrates the excellent fit of a single spectral line. The temperature and concentration of CO can be accurately evaluated in this spectral range only near room temperature, since in this range the CO spectrum contains rotational lines with rotational quantum numbers from $13 < J < 21$. These states correspond to the energies of the lower transition level, which are less than 886 cm^{-1}. At high temperatures the rotational lines

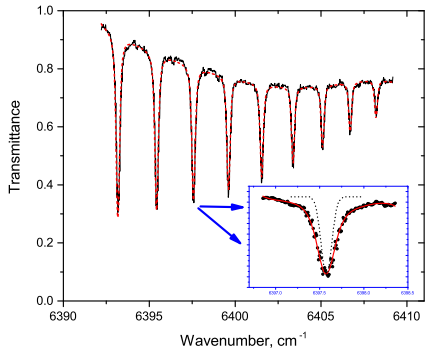

Fig. 3 Experimental (solid line) and simulated (dashed line) spectra of the CO molecule at room temperature. The inset depicts the R15 line at 6397.58 cm^{-1}. The dotted line in the inset shows the apparatus function of the spectrograph, approximated by a Gaussian. The concentration of CO was 2% in 1 atm of nitrogen at T = 298 K. The best fit results in a CO concentration of 1.9% and T = 302 K .

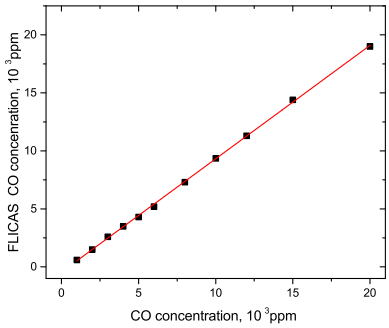

Fig. 4 Comparison of the CO concentrations extracted from spectral features with those defined by the mass flow controller at the room temperature.

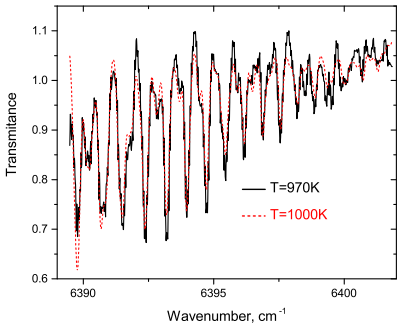

Fig. 5 The experimentally observed FLICAS spectrum of CO_2 recorded at 970K (solide line), along with a simulated CO_2 spectrum (dashed line). A CO_2 concentration of 50% at a total pressure of 1 atm was used in this experiment. The best fit yields 47% concentration at T=1000 K

in this range have nearly equal intensity, so are unsuitable for temperature evaluation.

Despite the difficulty in evaluating high temperatures using the CO molecule spectrum in this range, the CO concentration can still be evaluated accurately using independently measured temperature values. For instance, we can extract a temperature from the CO_2 spectrum, as elaborated below. In order to estimate the accuracy of the concentration evaluation, the fitting procedure was repeated for CO concentrations ranging from 0.1 % to 2 % of the mixture with nitrogen at atmospheric pressure. The results are depicted in Fig. 4. The lower limit of the CO concentrations used in this experiment is imposed not by the sensitivity of the detection method, but by the accuracy of the mass flow controller used for the CO gas supply. The signal-to-noise ratio at 2000 ppm CO concentration was about 5. That is, the CO concentration can be measured with the sensitivity of 400 ppm in this spectral range. Note that the sensitivity at room temperature can be better in a range near 6375 cm^{-1}.

In the 6390 - 6400 cm^{-1} spectral range, the CO_2 lines are very weak at room temperature. However, at elevated temperatures (above 400 K) these lines can be used for accurate temperature determination. Fig. 5 demonstrates a fit of the CO_2 spectrum recorded at 970K, and Fig. 6 summarizes the results of this method of temperature evaluation at various temperatures.

It must be noted that the temperature determination in experiments at high temperatures is affected by the temperature profile across the tubular oven (see fig. 2). Fortunately, CO_2 absorption in this spectral range drops fast as the temperature decreases, allowing us to evaluate the real optical length of the absorbing molecules at the nominal oven temperature. In order to evaluate to what extent the non-uniformity of temperature profile affects the effective temperature extracted from the CO_2 spectrum, we simulated this spectrum using HITRAN database and temperature profile shown in fig. 2. The obtained spectrum was further processed by the above described evaluation procedure. The extracted value of 952 K is rather close to the nominal value of 973 K. Thus, we can conclude that $\sim$30 K is a reasonable estimation for the accuracy of the uncertainty associated with the use of the "nominal" oven temperature values.

Fig. 6 compares the temperature evaluation from the FLICAS spectrum of CO_2 to the nominal oven temperature. This graph confirms that the accuracy of temperature measurements is about $\pm$50K over a wide range (300 - 1100 K). Again, this value includes the uncertainty in the thermal profile of the tubular oven. The sensitivity to CO_2 in the spectral range 6390 - 6400 cm^{-1} drops as the temperature increases, due to fast growth of its partition function. In situations where the CO_2 concentration is low, the temperature can be evaluated using the CO spectrum in the range of 6408 - 6418 cm^{-1}, to which the laser can be easily tuned.

This range includes the bandhead of the R-branch of the rovibrational CO spectrum. It contains CO lines with

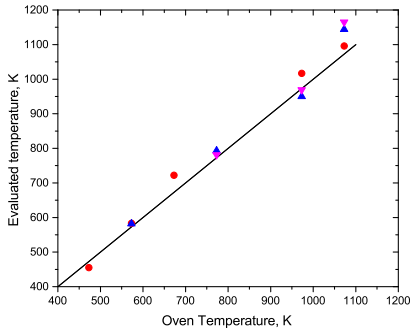

Fig. 6 Comparison of temperatures evaluated from the best fit CO_2 spectra and the nominal temperatures in the tubular oven. The temperature was evaluated at different concentrations (▼ −20 %, ▲ −40%, ● −50%)

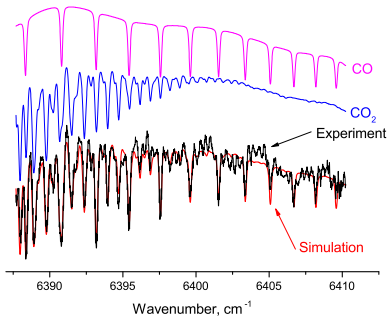

Fig. 7 Experimental and best-fit simulated FLICAS spectra of the CO/CO_2 mixture (1%/50%) at an oven temperature of 773 K. The best fit yields the following results: [CO]=1%, [CO_2=53%, T=767K

rotational quantum numbers from J=21 to J=47, corresponding to low-level transition energies E= 886 to 4300 cm^{-1}. This range has good temperature sensitivity at high temperatures. Note that the temperature and the CO concentration can be evaluated simultaneously in this spectral range.

Fig. 7 depicts the results of an experiment where we heated a mixture of 50% CO_2 and 1%CO at 1 atm pressure to a temperature of 773 K. The fitting program utilized the HITRAN database for CO lines and the HITEMP database for CO_2 lines. It optimized the following parameters: temperature, concentrations of CO and CO_2, and coefficients of the polynomial that fits the baseline. Despite the overlap between CO and CO_2 spectral lines it was possible to perform a rather accurate simultaneous determination of the temperature (the fit yields T = 767 K) and concentrations of CO (the fit yields 1.0%) and CO_2 (the fit yields 53%). This demonstrates the possibility of simultaneous temperature and concentration extraction from a measured multi-species spectrum. It must be noted that increasing the CO concentration somewhat degrades the accuracy of the temperature determination at high temperatures, due to the weak temperature dependence of the CO spectrum in this spectral range.

The 6390 - 6410 cm^{-1} spectral range also allows measurement of the methane spectrum at relatively low temperatures The intensity of the spectrum is not very high, since the most intense lines are located near 6430 cm^{-1}, within the spectral range achievable with our laser. Nevertheless, the ability to measure the methane concentration together with CO and CO_2 is of interest for several applications such as monitoring combustion completeness and natural gas reforming. The main problem with measuring concentration and temperature together based on the FLICAS spectrum of the CH_4 molecule is that the methane spectrum is very complex and the lines may lack full assignment, especially for energies in the lower transition levels.

Fig. 8 depicts the spectra of the water lines observed in

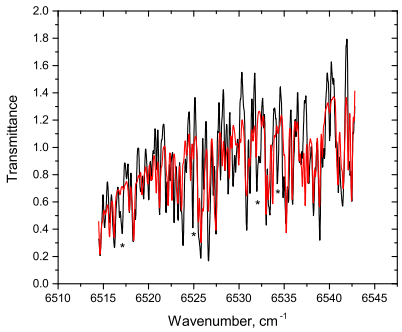

Fig. 8 FLICAS spectra of water in metane/air adiabatic flame with eqvivalence ratio ϕ= 1.1(black line) with their best-fit simulations (red line). The simulation yields the temperature of 2090K, and the evaluation using a model based on the detailed chemical mechanism yields 2200K. The features observed in the experimental spectrum and missing in the HITRAN database are shown by the asterisks.

methane/air flame with equivalence ratio ϕ=1.1. The water spectrum is very complex, HITRAN database contains extensive data concerning the H_2O spectrum at high temperatures (HITEMP2010). Fitting the spectra with use of the procedure described above results in the temperature T= 2090 K, which is close to the calculated adiabatic temperature of 2200 K. Nevertheless, some features of the experimental FLICAS spectrum of H_2O do not correlate well to the HITRAN database data. The work aimed to clarification of this issue is currently in the progress.

4 Conclusions

Fiber laser intracavity absorption spectroscopy (FLICAS) was used to simultaneously measure temperature, CO concentration, and CO_2 concentration in the temperature range 296 - 1200 K. The temperature can be measured using CO_2 lines in the 6390 - 6410 cm^{-1} range or or using CO spectral lines in the vicinity of the bandhead

(6408 - 6418 cm^{-1} range). The sensitivity to CO is about 400 ppm at room temperature and about 0.2% at 1200K. The sensitivity to CO_2 is between 1 - 10% depending on temperature. This range of sensitivities makes FLICAS sensors suitable for many applications, although it can be improved at least an order of magnitude by increasing the generation time.

The main advantages of FLICAS measurements are the possibility of simultaneously measuring CO, CO_2 and temperature in a very short time (3.7 μs in this work, without averaging) and operating under conditions of strong broadband absorption or light scattering, which are common in flames and other harsh environments. Accurate absolute concentration measurements demand knowledge of the optical path length. When this cannot be easily determined, calibration against known concentrations is required.

5 Acknowledgements

This work was supported in part by the Israel Science Foundation (Grant No. 1149/12), Israel Ministry of Energy and Water Resources (Grant No. 211-11-007/2011-7-10) and the Research Authority of The Open University of Israel (GrantNo. 47324).

References

1 D. R. Crawford, M. E. Parrish, D. L. Gee, C. N. Harward, Intra-puff CO and CO_2 measurements of cigarettes with iron oxide cigarette paper using quantum cascade laser spectroscopy, Spectrochim. Acta A 67 (1) (2007) 4–15. doi:10.1016/j.saa.2006.10.035.

2 S. A. Diddams, L. Hollberg, V. Mbele, Molecular fingerprinting with the resolved modes of a femtosecond laser frequency comb, Nature 445 (7128) (2007) 627–630. doi:10.1038/nature05524.

3 E. Furlong, R. Mihalcea, M. Webber, D. Baer, R. Hanson, Diode-laser sensors for real-time control of pulsed combustion systems, AIAA J. 37 (6) (1999) 732–737. doi:10.2514/2.781.

4 R. Mihalcea, D. Baer, R. Hanson, Diode laser sensor for measurements of CO, CO_2, and CH_4 in combustion flows, Appl. Opt. 36 (33) (1997) 8745–8752. doi:10.1364/AO.36.008745.

5 D. Sonnenfroh, M. Allen, Observation of CO and CO_2 absorption near 1.57 μm with an external-cavity diode laser, Appl. Opt. 36 (15) (1997) 3298–3300. doi:10.1364/AO.36.003298.

6 A. Thompson, H. Northern, B. Williams, M. Hamilton, P. Ewart, Simultaneous detection of CO_2 and CO in engine exhaust using multi-mode absorption spectroscopy, MUMAS, Sensors Actuators B 198 (2014) 309–315. doi:10.1016/j.snb.2014.03.060.

7 E. Vargas-Rodriguez, H. N. Rutt, Design of CO, CO_2 and CH_4 gas sensors based on correlation spectroscopy using a Fabry-Perot interferometer, Sensors Actuators B 137 (2) (2009) 410–419. doi:10.1016/j.snb.2009.01.013.

8 R. M. Spearrin, W. Ren, J. B. Jeffries, R. K. Hanson, Multi-band infrared CO_2 absorption sensor for sensitive temperature and species measurements in high-temperature gases, Appl. Phys. B 116 (4) (2014) 855–865. doi:10.1007/s00340-014-5772-7.

9 A. Sane, A. Satija, R. Lucht, J. Gore, Simultaneous co concentration and temperature measurements using tunable diode laser absorption spectroscopy near 2.3 μm, Appl.Phys.B. 117 (2014) 7 – 18.

10 D. Baer, R. Hanson, M. Newfield, N. Gopaul, Multiplexed diode-laser sensor system for simultaneous H_2O, CO_2 and temperature-measurements, Opt. Lett. 19 (22) (1994) 1900–1902. doi:10.1364/OL.19.001900.

11 D. Oh, M. Paige, D. Bomse, Frequency modulation multiplexing for simultaneous detection of multiple gases by use of wavelength modulation spectroscopy with diode lasers, Appl. Opt. 37 (12) (1998) 2499–2501. doi:10.1364/AO.37.002499.

12 R. M. Spearrin, C. S. Goldenstein, I. A. Schultz, J. B. Jeffries, R. K. Hanson, Simultaneous sensing of temperature, CO, and CO2 in a scramjet combustor using quantum cascade laser absorption spectroscopy, Appl. Phys. B 117 (2) (2014) 689–698. doi:10.1007/s00340-014-5884-0.

13 W. Denzer, G. Hancock, M. Islam, C. E. Langley, R. Peverall, G. A. D. Ritchie, D. Taylor, Trace species detection in the near infrared using Fourier transform broadband cavity enhanced absorption spectroscopy: initial studies on potential breath analytes, Analyst 136 (4) (2011) 801–806. doi:10.1039/c0an00462f.

14 K. Divya, K. Sulochana, N. J. Vasa, Superluminescent Diode-Based Multiple-Gas Sensor for NH3 and H2O Vapor Monitoring, IEEE J. Select. Top. Quant. Electron. 18 (5) (2012) 1540–1546. doi:10.1109/JSTQE.2011.2179021.

15 V. Baev, T. Latz, P. Toschek, Laser intracavity absorption spectroscopy, Appl. Phys. B. 69 (3) (1999) 171–202.

16 A. Campargue, F. Stoeckel, M. Chenevier, High sensitivity intracavity laser spectroscopy: applications to the study of overtone transitions in the visible range., Spectrochimica Acta Rev. 13 (1) (1990) 69–88.

17 S. Cheskis, A. Goldman, Laser diagnostics of trace species in low-pressure flat flame, Prog. Energ. Comb .Sci. 35 (4) (2009) 365–382. doi:10.1016/j.pecs.2009.02.001.

18 I. Rahinov, A. Goldman, S. Cheskis, Intracavity laser absorption spectroscopy and cavity ring-down spectroscopy in low-pressure flames, Appl. Phys. B. 81 (1) (2005) 143–149.
URL ISI:000230033800021

19 A. Goldman, I. Rahinov, S. Cheskis, B. Lohden, S. Wexler, K. Sengstock, V. M. Baev, Fiber laser intracavity absorption spectroscopy of ammonia and hydrogen cyanide in low pressure hydrocarbon flames, Chem. Phys. Lett. 423 (1-3) (2006) 147–151.

20 B. Loehden, S. Kuznetsova, K. Sengstock, V. M. Baev, A. Goldman, S. Cheskis, B. Palsdottir, Fiber laser intracavity absorption spectroscopy for in situ multicomponent gas analysis in the atmosphere and combustion environments, Appl. Phys. B 102 (2) (2011) 331–344. doi:10.1007/s00340-010-3995-9.

21 A. Goldman, S. Cheskis, Intracavity laser absorption spectroscopy of sooting acetylene/air flames, Applied Physics B to be published.

22 I. Rahinov, A. Fomin, M. Poliak, S. Cheskis, Absorption electronic spectrum of gaseous FeO: in situ detection with intracavity laser absorption spectroscopy in a nanoparticle-generating flame reactor, Appl. Phys. B 117 (1) (2014) 317–323. doi:10.1007/s00340-014-5838-6.

23 J. Hunkemeier, R. Bohm, V. Baev, P. Toschek, Spectral dynamics of multimode nd3+- and yb3+-doped fibre lasers with intracavity absorption, Opt. Commun. 176 (4-6) (2000) 417–428.
URL ISI:000086357200017

24 L. S. Rothman, I. E. Gordon, Y. Babikov, A. Barbe, D. C. Benner, P. F. Bernath, M. Birk, L. Bizzocchi, V. Boudon, L. R. Brown, A. Campargue, K. Chance, E. A. Cohen, L. H. Coudert, V. M. Devi, B. J. Drouin, A. Fayt, J. M. Flaud, R. R. Gamache, J. J. Harrison, J. M. Hartmann, C. Hill, J. T. Hodges, D. Jacquemart, A. Jolly, J. Lamouroux, R. J. Le Roy, G. Li, D. A. Long, O. M. Lyulin, C. J. Mackie, S. T. Massie, S. Mikhailenko, H. S. P. Mueller, O. V. Naumenko, A. V. Nikitin, J. Orphal, V. Perevalov, A. Perrin, E. R. Polovtseva, C. Richard, M. A. H. Smith, E. Starikova, K. Sung, S. Tashkun, J. Tennyson, G. C. Toon, V. G. Tyuterev, G. Wagner, The HITRAN2012 molecular spectroscopic database, J. Quant. Spect. Radiat. Trans. 130 (SI) (2013) 4–50. doi:10.1016/j.jqsrt.2013.07.002.

25 L. S. Rothman, I. E. Gordon, R. J. Barber, H. Dothe, R. R. Gamache, A. Goldman, V. I. Perevalov, S. A. Tashkun, J. Tennyson, HITEMP, the high-temperature molecular spectroscopic database, J. Quant. Spect. Radiat. Trans. 111 (15, SI) (2010) 2139–2150. doi:10.1016/j.jqsrt.2010.05.001.